Resource

TRANSPARENT PROCESS OPEN ACCESS

THE EMBO JOURNAL

Discrete domains of gene expression in germinal layers distinguish the development of gyrencephaly

Camino de Juan Romero[1], Carl Bruder[2,†], Ugo Tomasello[1], José Miguel Sanz-Anquela[3] & Víctor Borrell[1,*]

Abstract

Gyrencephalic species develop folds in the cerebral cortex in a stereotypic manner, but the genetic mechanisms underlying this patterning process are unknown. We present a large-scale transcriptomic analysis of individual germinal layers in the developing cortex of the gyrencephalic ferret, comparing between regions prospective of fold and fissure. We find unique transcriptional signatures in each germinal compartment, where thousands of genes are differentially expressed between regions, including ~80% of genes mutated in human cortical malformations. These regional differences emerge from the existence of discrete domains of gene expression, which occur at multiple locations across the developing cortex of ferret and human, but not the lissencephalic mouse. Complex expression patterns emerge late during development and map the eventual location of folds or fissures. Protomaps of gene expression within germinal layers may contribute to define cortical folds or functional areas, but our findings demonstrate that they distinguish the development of gyrencephalic cortices.

Keywords folding; lissencephaly; microarray; protocortex; transcription factor
Subject Categories Development & Differentiation; Neuroscience
DOI 10.15252/embj.201591176 | Received 4 February 2015 | Revised 26 March 2015 | Accepted 27 March 2015 | Published online 27 April 2015
The EMBO Journal (2015) 34: 1859–1874

See also: **M Albert & WB Huttner** (July 2015)

Introduction

The mammalian cerebral cortex is divided into multiple anatomical and functional areas, and in higher mammals, it is further subdivided into folds and fissures. Cortical areas and cortical folds form during embryonic development from the cortical anlage in highly stereotyped patterns, suggesting a strong genetic regulation (Borrell & Reillo, 2012). A limited number of transcription factors have been identified to control the size, position, and area identities of cortical subdivisions, including *Pax6*, *Lhx2*, *Emx2*, and *Sp8* (Bishop *et al*, 2000; Yun *et al*, 2001; Sahara *et al*, 2007; Mangale *et al*, 2008; Chou *et al*, 2009). Despite the subdivision of the mature cerebral cortex into discrete structural/functional units, these transcription factors controlling regional fate are expressed in gradients across such subdivisions in the embryonic cortical germinal layers, raising the question of how the latter are implemented.

Small enhancer elements have been recently identified to drive reporter gene expression in discrete modules, or protodomains, of the embryonic cerebral cortex (Visel *et al*, 2013; Pattabiraman *et al*, 2014). These enhancers integrate broad transcriptional information, including expression of several of the transcription factors regulating cortical patterning, to activate gene expression in protodomains (Nord *et al*, 2013; Pattabiraman *et al*, 2014). Variations in such small enhancer elements may be at the core of cortical patterning during development and evolution (Bae *et al*, 2014; Borrell & Gotz, 2014). However, the delineation of discrete cortical subdivisions must require that effector genes (i.e., cell cycle regulators, cell fate determinants, neuron terminal selectors; or their interfering RNAs) (Dehay & Kennedy, 2007; Molyneaux *et al*, 2007; Hobert, 2011; Bae *et al*, 2014) be expressed in protodomains along the embryonic germinal layers.

During cortical development, progenitor cells are organized in germinal layers, namely the ventricular zone (VZ) and the subventricular zone (SVZ) (Borrell & Gotz, 2014). In gyrencephalic species (with a folded cerebral cortex), the SVZ is extraordinarily large and split into inner (ISVZ) and outer subventricular zone (OSVZ) (Smart *et al*, 2002). The outstanding diversity of progenitor cell types in the OSVZ and their amplificative potential is considered central for cortical expansion and folding (Lui *et al*, 2011; Betizeau *et al*, 2013; Borrell & Gotz, 2014). Previous work has demonstrated that, in the gyrencephalic ferret, local overexpression in OSVZ of the cell cycle-promoting genes *Cdk4* and *CyclinD1* increases cortical surface area and folding, whereas reduction in cell proliferation in OSVZ has the opposite effect (Reillo *et al*, 2011; Nonaka-Kinoshita *et al*, 2013). In spite of such robust experimental phenotypes, naturally occurring patterns of gene expression in germinal layers supporting the stereotyped development of cortical folds, or discrete cortical areas, have not been reported.

To identify genes whose expression co-varies with the stereotypic patterning of the cerebral cortex, here we have performed a large-scale

1 Instituto de Neurociencias, Consejo Superior de Investigaciones Científicas & Universidad Miguel Hernández, Sant Joan d'Alacant, Spain
2 Department of Microbiology, Tumor and Cell Biology, Karolinska Institutet, Stockholm, Sweden
3 Service of Pathology, Hospital Universitario "Principe de Asturias", Alcalá de Henares, Spain
*Corresponding author. Tel: +34 965 919245; E-mail: vborrell@umh.es
†Present address: GeneData AG, Basel, Switzerland

differential expression screen of germinal layers in the ferret cortex, distinguishing between a region prospective of fold (splenial gyrus, SG) and its prospective adjacent fissure (lateral sulcus, LS). Our analysis demonstrates a remarkable genetic heterogeneity between and within each germinal layer along the ferret cortex, where our microarray data indicate the differential expression of thousands of genes between prospective gyrus and sulcus. These differences emerge from the existence of domains exhibiting significantly different gene expression levels. Remarkably, these domains or modules are present in the gyrencephalic ferret and human but not in the lissencephalic mouse cortex. In ferret, modules of gene expression are obvious at multiple locations throughout the developing cortex, systematically mapping the prospective location of folds or fissures, particularly in the OSVZ. Importantly, our screen highlights a majority of genes mutated in human cortical malformations (Barkovich *et al*, 2012), which also display modular expression, highlighting the promise of our screen as an entry point to identifying novel genes potentially mutated in human malformations of cortical development.

Results

Genetic screen of cortical regions

To investigate the genetic regulation of cortical patterning, including folding, we focused on the naturally gyrencephalic ferret and analyzed the transcriptomic content of the three main cortical germinal layers: VZ, ISVZ, and OSVZ. These zones were individually microdissected from living brain slices at P2, 1 week prior to the morphological distinction of these folds, and sampled separately in the prospective splenial gyrus (SG) and its flanking lateral sulcus (LS) (Fig 1A–E) (Smart & McSherry, 1986a). Using a ferret-specific microarray (Camp *et al*, 2012), we screened for differentially expressed genes (DEGs) whose expression level varied more than two fold ($P < 0.05$, fold change (FC) > 2) between (i) cortical areas along individual germinal layers, (ii) germinal layers within individual cortical areas, and (iii) in both axes (Fig 1F–H). To identify the main source of variability in our microarray data, we performed principal component analysis (PCA) and analysis of variance distribution across our datasets. PCA confirmed that the primary source of variability was caused by differences between germinal layers and cortical areas, with a minor contribution from biological replicates (Supplementary Fig S1C).

Due to the location of the ISVZ, intercalated between VZ and OSVZ, we expected to find in this layer the highest experimental noise and inter-sample variability, and hence the smallest number of genes with statistically different expression. Whereas our microarray data revealed the ISVZ to have the fewest DEGs, sample variance analyses also demonstrated that this layer actually had overall the lowest variability, which was similar in SG and LS (Supplementary Fig S1E). Differences in gene expression levels revealed by our various microarray data screens were validated and confirmed by qRT–PCR (24 genes; Supplementary Tables S1, S4 and S5) and *in situ* hybridization (ISH; 20 genes), giving us high confidence in our custom-made ferret-specific microarray. Altogether, this supported the validity of our experimental design for transcriptomic profiling of individual germinal layers and prospective cortical areas in the developing ferret cortex.

Germinal layers have different transcriptional fingerprints between SG and LS

To investigate the contribution of cortical progenitor genetics on the distinction between SG and LS, we searched for transcriptomic differences between these two areas within each germinal layer (Fig 1F). Remarkably, although SG and LS are nearly adjacent, we identified 2,218 DEGs between them, most being differentially expressed along one of the germinal layers only (Figs 1F, 2A and B and Supplementary Fig S1A and B). The OSVZ contained the largest number of DEGs (1,194), where > 90% had higher expression levels in SG, whereas in VZ, ~60% were more expressed in LS (Fig 2B and Supplementary Fig S1D). In ISVZ, we found the fewest number of DEGs (678). Microarray results were validated for a selection of genes by qRT–PCR using ferret-specific primers, and also by *in situ* hybridization (ISH) using ferret-specific probes (Fig 2C and D, and Supplementary Tables S1 and S2). ISH stains confirmed that expression levels of individual genes changed significantly between SG and LS at least in one germinal layer, while frequently showing similar expression levels in other layers. These results establish that our ferret-specific microarray can be successfully used to identify genetic programs regulating regional differences along cortical germinal layers (Fig 2E). Importantly, DEGs between prospective SG and LS included genes known to be important in cortical patterning in mouse, including *Nefl* and *Cdh8*, further supporting that differential gene expression along germinal layers between prospective SG and LS may contribute to cortical patterning.

Our observation that the largest number of DEGs between SG and LS was found in the OSVZ is consistent with the notion that progenitor cells in this layer play central roles in the expansion and folding of the cerebral cortex (Fietz & Huttner, 2011; Lui *et al*, 2011; Reillo *et al*, 2011; Borrell & Reillo, 2012). To identify the biological processes in which these DEGs are involved, we performed gene ontology (GO) analysis. The categories most highly represented were common to all three germinal layers and included regulation of transcription, cell adhesion, extracellular matrix, cytoskeleton, and cell cycle (i.e., *Cdk4*, *CyclinD1*; Fig 2F), all directly related to regulating the proliferation of the various types of cortical progenitor cells and their lineage relationships (Gotz & Huttner, 2005; Fietz *et al*, 2010; Lui *et al*, 2011; Borrell & Reillo, 2012). Among these, the Notch, Wnt, MAPK, and Shh signaling pathways are well-known central regulators of cortical progenitor cells. A targeted search highlighted DEGs belonging to these pathways in all germinal layers (Supplementary Fig S2 and Supplementary Table S3). Importantly, these DEGs always included the read-out genes of each cascade, thus confirming the differential activation of the entire pathway. Taken together, our analyses indicated that the transcriptional regulation of cortical germinal layers and their lineage relationships is different between the prospective splenial gyrus and lateral sulcus.

Next, we screened for DEGs between germinal layers, while distinguishing between SG and LS (Figs 1G, 3A and B). The number of DEGs (542) was much smaller than when comparing between SG and LS, which was unexpected given the notorious differences in cytoarchitecture and cell composition between germinal layers, as opposed to their apparent similarity across SG and LS (Reillo *et al*, 2011; Reillo & Borrell, 2012). Although LS had a larger number of DEGs (Fig 1G), the mean FC value was higher or similar in SG than in LS for all comparisons (Supplementary Fig S1F and I). DEGs in

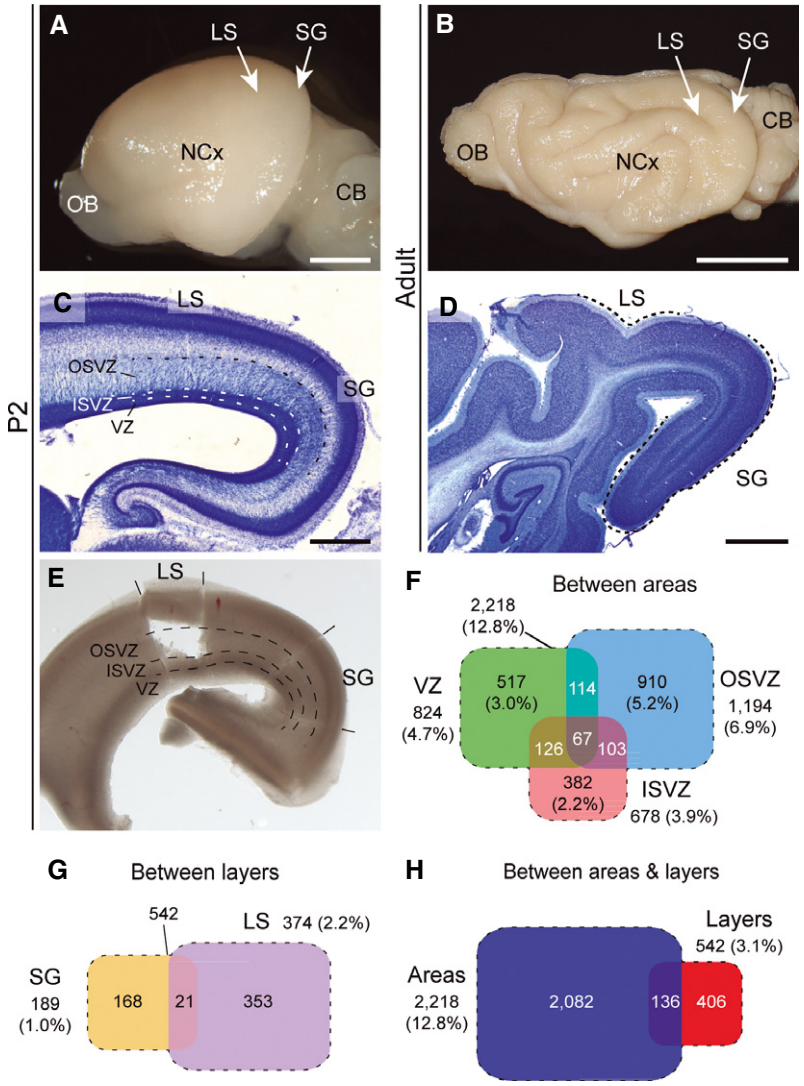

Figure 1. Stereotyped cortical folding and sampling strategy.

A–D Lateral external view (A,B) and Nissl stain of sagittal sections (C,D) of P2 and adult ferret brains showing the location and extent (dashed lines in D) of the fully developed, or prospective lateral sulcus (LS) and splenial gyrus (SG). Note the absence of cortical folding at P2, where VZ, ISVZ, and OSVZ are identifiable. CB, cerebellum; NCx, neocortex; and OB, olfactory bulb. Scale bars, 500 μm (A), 1 cm (B), 1 mm (C), and 2 mm (D).

E Example of a living brain slice at P2, from where OSVZ, ISVZ, and VZ in LS and SG were microdissected (lines).

F–H Venn diagrams representing the abundance of genes differentially expressed (DEGs: $P < 0.05$, FC ≥ 2) between the cortical areas SG and SL within each germinal layer (F), between germinal layers within each cortical area (G) and between cortical areas and germinal layers simultaneously (H). Numbers of genes differentially expressed in only one of the groups, simultaneously in two or three of them, and total in each group, are indicated. The percentage of genes differentially expressed with respect to all genes expressed in these tissues is also indicated.

both regions followed two distinct patterns of abundance: for most DEGs, transcript abundance followed a trend progressively increasing or decreasing from VZ to OSVZ. Increasing from VZ to OSVZ was typical of SG, whereas decreasing tendency was typical of LS (Fig 3C–H, Supplementary Table S4). Such differences between these two regions were further highlighted by the fact that the vast majority (96.1%) of the 542 DEGs between layers were differentially expressed in one region but not the other (Fig 1H). For a minority of genes, differences in expression levels were layer-specific, where only one of the layers had significantly different expression levels than the other two. ISVZ-specific genes (similar expression in VZ and OSVZ, but different in ISVZ) were extremely rare or absent (Fig 3E and F). FC values for DEGs in VZ-ISVZ and ISVZ-OSVZ comparisons were much smaller than for DEGs between VZ and OSVZ, in both cortical areas (Supplementary Fig S1F, G and I). Together, this suggested that the ISVZ expresses a transcriptional signature intermediate between VZ and OSVZ.

Unsupervised hierarchical clustering of DEGs indicated that in both cortical regions, the OSVZ displayed the most different transcriptional fingerprint (Fig 3C and D). This is in full agreement with previous reports indicating that progenitor cells in the OSVZ are likely unique in their playing key roles in cortical development (Smart *et al*, 2002; Fietz *et al*, 2010; Fietz & Huttner, 2011; Lui *et al*, 2011; Reillo *et al*, 2011; Borrell & Reillo, 2012). Intriguingly, previous

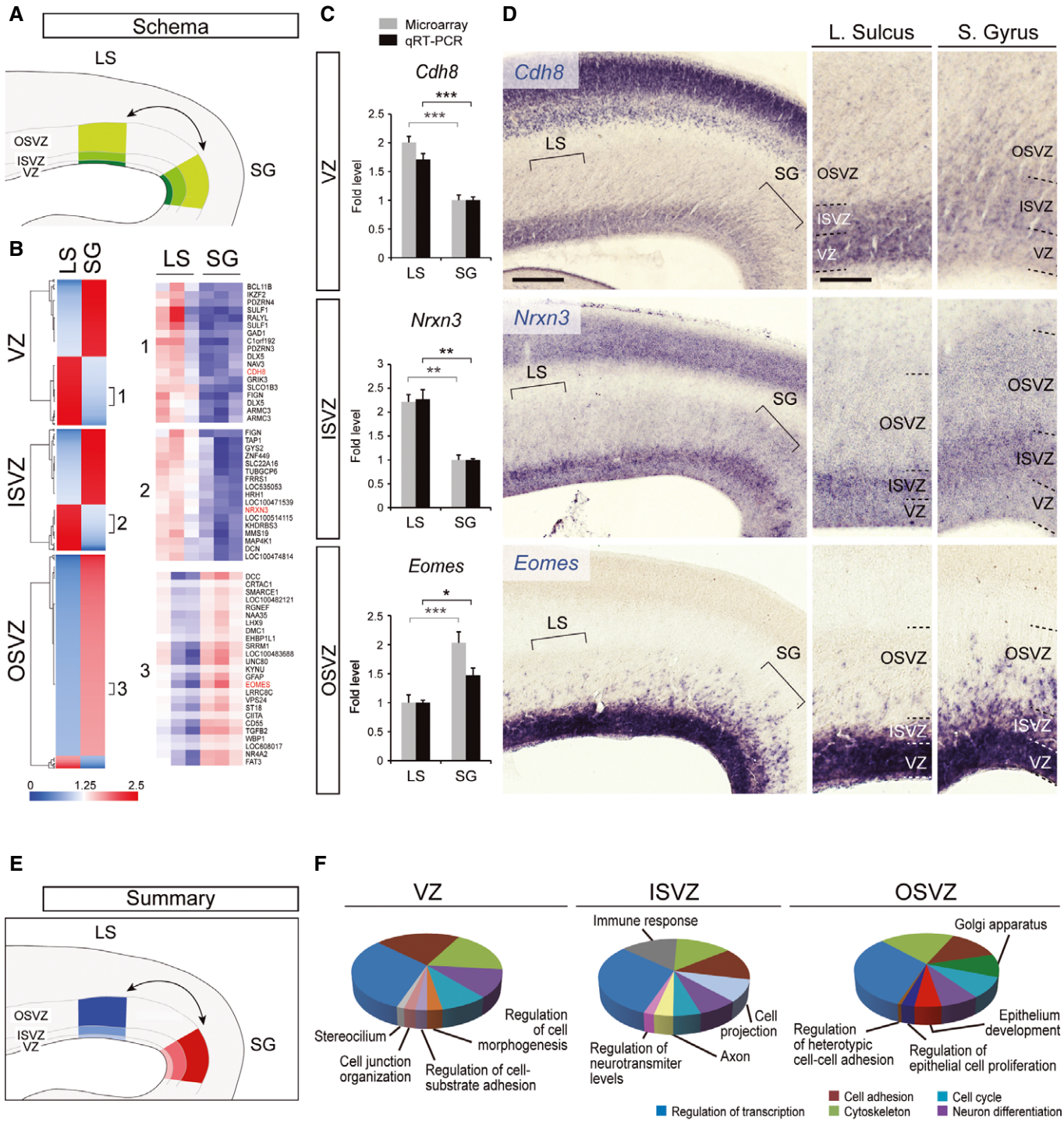

Figure 2. Differential gene expression between splenial gyrus and lateral sulcus along germinal layers.

A Experimental paradigm: prospective lateral sulcus (LS) and splenial gyrus (SG) were compared within each germinal layer.

B Heatmap of unsupervised hierarchical clustering of DEGs ($P < 0.05$, $\geq$ 2-fold difference) between LS and SG within each germinal layer. Color-coded scale bar indicates fold level of expression relative to average. Original triplicate data from the selected three gene clusters are shown.

C, D Validation of microarray data by qRT–PCR and *in situ* hybridization. Plots are mean + SEM of relative fold level. Student's *t*-test, $*P < 0.05$, $**P < 0.01$, $***P < 0.001$. Statistical significance is indicated for qRT–PCR (black) and microarray (gray) data. Note that intensity of stains varies in the indicated germinal layer, and that signal intensity for *Cdh8* and *Nrxn3* in OSVZ displays a pattern opposite to VZ and SVZ. ISH patterns were observed in 2–3 animals, at least three sections per animal, for each gene. Scale bars, 500 μm (view); 200 μm (detail).

E Summary schema of results: most DEGs had higher expression in SG than in LS, particularly in OSVZ.

F Pie charts of significantly enriched GO terms associated with DEGs between LS and SG in each germinal layer. Terms in legend are common to all layers and among the most represented.

transcriptomic analyses of human cortical germinal zones concluded that VZ is the most different germinal zone, while ISVZ and OSVZ are relatively similar to each other (Fietz *et al*, 2012). GO analysis of DEGs in our microarray dataset revealed that some of the most highly enriched categories among DEGs between germinal layers were common to both SG and LS, including regulation of transcription, cell adhesion, extracellular matrix, cytoskeleton, and neuron differentiation, as previously also found in the human embryo cortical germinal zones (Fietz *et al*, 2012). In contrast, other categories were specific to only one region. Of these, GO terms in LS were mostly related to cell cycle and cell junction, whereas intriguingly in SG, they were mostly related to cell–cell signaling and synapse function (Fig 3I).

To further understand the distinctions between cortical areas and germinal zones, we probed our dataset to identify genes differentially expressed simultaneously across both axes ($P < 0.05$, FC ≥ 2 between at least two groups). Two-way ANOVA identified 136 DEGs (Figs 1H and 4, Supplementary Table S5), which were then used to assess the transcriptional similarity between zones. Microarray results were validated for a selection of genes by qRT–PCR using ferret-specific primers, and also by *in situ* hybridization (ISH) using ferret-specific probes (Fig 4C and D, and Supplementary Tables S2 and S5). Unsupervised hierarchical clustering and Pearson's correlation matrices revealed that VZ and ISVZ within each area share the highest similarities, whereas OSVZ of the SG is by far the most different of the six germinal zones (Fig 4A and B, and Supplementary Table S5).

Taken together, our analyses indicated that the transcriptional regulation of cortical progenitor cells, particularly of those genes most directly implicated in regulating proliferative dynamics and lineage relationships, is different between the prospective SG and LS. Our results also supported the notion that the OSVZ plays uniquely central roles in the development and patterning of cortical folds (Fietz & Huttner, 2011; Lui *et al*, 2011; Reillo *et al*, 2011; Borrell & Reillo, 2012), seemingly by imprinting regional heterogeneity along the cortical anlage.

Cortical progenitor domains in gyrencephalic brains

The above analyses demonstrated that in germinal layers of the developing gyrencephalic ferret cortex, gene expression levels change quite dramatically between nearly adjacent regions. This is reminiscent of the embryonic spinal cord, where gene expression in the VZ is sharply parcellated to define the types of neurons generated from individual germinal domains (Jessell, 2000). This prompted the idea that in germinal layers of the ferret cortex, gene expression may occur in modular patterns, where specific cortical domains are distinguished by significantly different gene expression levels. To test this notion, we extended our ISH analysis of DEGs between SG and LS, to span across the cortical region covering these two areas (Fig 5A). As predicted, for many of the genes analyzed, changes in expression levels were not softly gradual but quite abrupt, in steep gradients, delimiting distinct gene expression domains. For some genes, these domains were obvious in only one layer, most frequently OSVZ (i.e., *Fgfr2*, *Lhx2*, *Eomes*, *Cdk6*) but also VZ (i.e., *Cdh8*), while in the other layers, the same gene was expressed homogeneously or in a continuous gradient, which demonstrated the specificity of these modular gene expression patterns (Fig 5A). For other genes, short-range changes occurred in multiple layers, but usually at different locations in each layer (i.e., *Fgfr3*; Fig 5A).

The location and extent of domains in OSVZ correlated remarkably well with the location of the prospective SG and LS. Significantly, genes expressed in domains included *Trnp1*, known to induce gyrification in mice upon experimental reduction in its expression in VZ locally (Stahl *et al*, 2013). In agreement with this notion, endogenous *Trnp1* expression in ferret was significantly lower in SG compared to LS along the VZ, while in the other layers, the change was gradual (Fig 5A). Together, this demonstrated the specificity of these expression patterns and supported the notion of their having functional relevance in cerebral cortex patterning in ferret. This idea was further substantiated by analyses in the developing mouse cortex at equivalent developmental stages, where the same genes were found expressed homogeneously or in long-range shallow gradients (Fig 5B). Therefore, modular gene expression may be relevant for cortical patterning in gyrencephalic species.

Since SG and LS are located in visual areas A17 and A19 (Law *et al*, 1988; Manger *et al*, 2002), we next asked whether the domains of gene expression in OSVZ might map area identity versus folding (Elsen *et al*, 2013). Because each cerebral hemisphere has only one A17 and one A19, but multiple folds and fissures, if domains of expression for a set of genes occurred only once these might define the identity of a specific cortical area, but if they occurred multiple times, they might define cortical folds instead. Examination of expression patterns for *Fgfr3*, *Cdk6*, and *Eomes* in OSVZ along the entire rostro-caudal and latero-medial extent of the developing cortex revealed distinct domains of high and low levels at multiple locations, outlining complex maps across the early postnatal cerebral cortex (Fig 6). This seemed largely incompatible with the idea that

Figure 3. Differential gene expression between germinal layers in SG and LS.

A, B Experimental paradigms: the three germinal layers were compared pair-wise within the prospective SG (A) and LS (B) following ANOVA analysis.

C, D Heatmaps of unsupervised hierarchical clustering of DEGs ($P < 0.05$, ≥ 2 FC) between germinal layers within SG (C) and LS (D). Color-coded scale bars indicate fold level of expression relative to average.

E, F Original triplicate data from a selection of gene clusters with typical tendency patterns (clusters 1 and 2) or layer-specific patterns (clusters 3). Representative validated genes are named in red.

G Validation of microarray data by qRT–PCR and ISH for DEGs in SG (top) and LS (bottom). Plots are mean + SEM of relative fold level. Student's *t*-test, $*P < 0.05$, $**P < 0.01$, $***P < 0.001$. Scale bar, 200 μm.

H Summary schema of results: in SG, gene expression levels for the majority of DEGs increased dramatically from VZ through OSVZ; in LS, fold differences were smaller and followed the opposite tendency.

I Pie charts of significantly enriched GO terms associated with DEGs between layers. Terms in legend are common to both areas and are among the most represented.

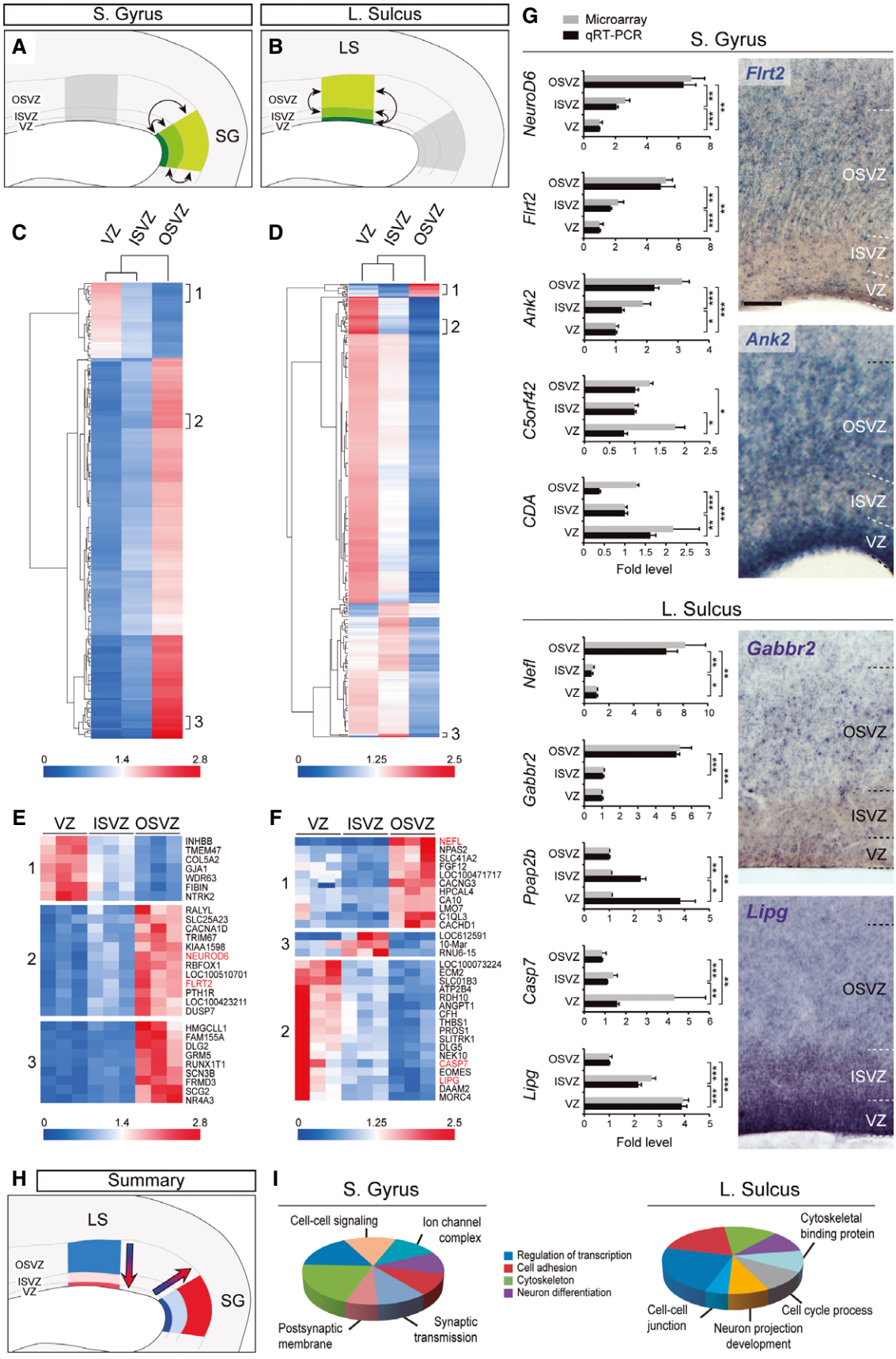

Figure 3.

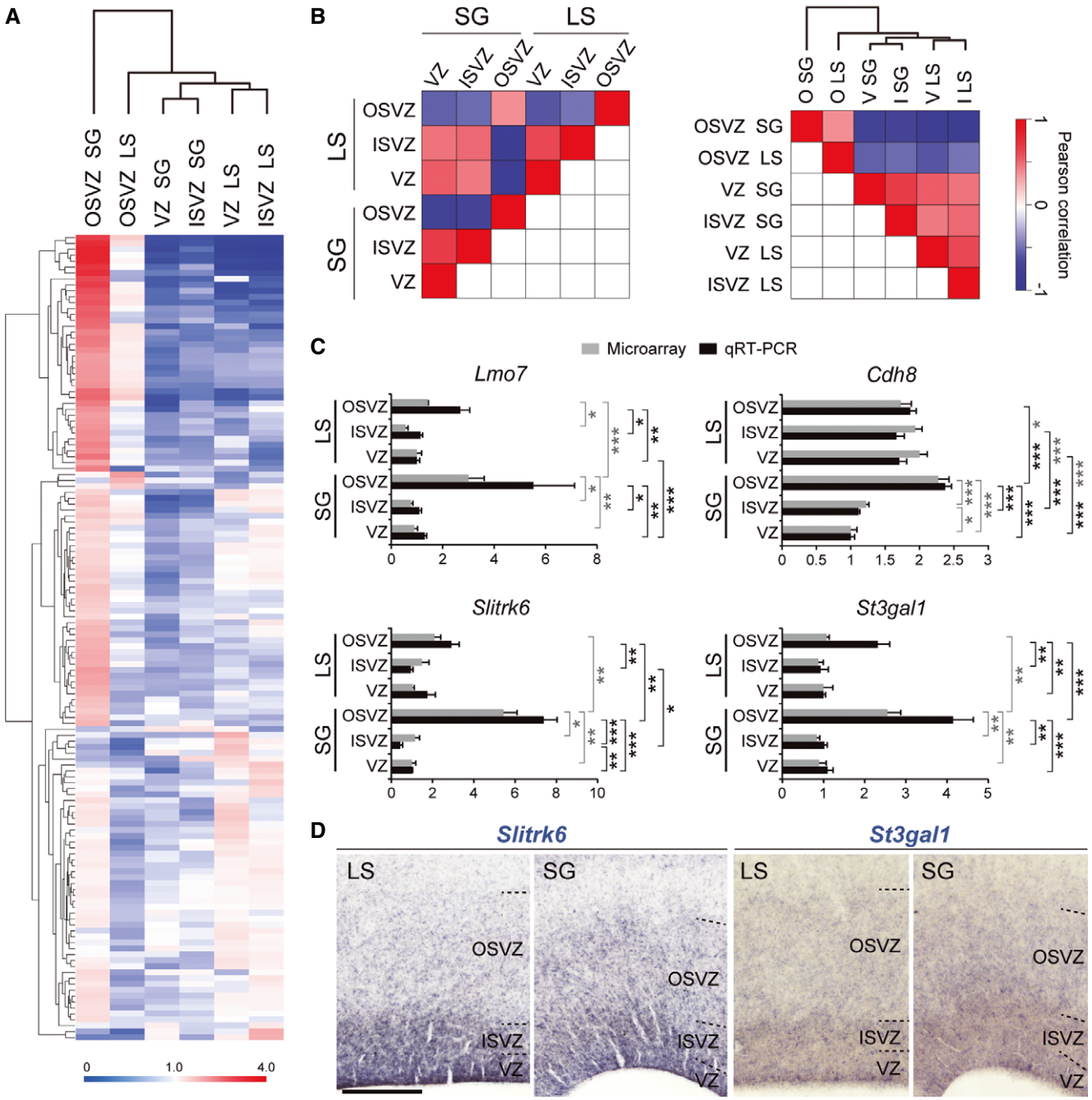

Figure 4. Genes differentially expressed between both SG-LS and germinal layers.

A Heatmap of unsupervised hierarchical clustering of DEGs ($P < 0.05$, ≥ 2 FC) between germinal layers and cortical areas. Color-coded scale bar indicates fold level of expression relative to average.

B Heatmap matrices of pair-wise Pearson correlations between germinal zones, and unsupervised hierarchical clustering, with dendrogram representing similarity relationships between germinal zones in Euclidian space. OSVZ in SG is the most dissimilar germinal zone, whereas VZ and ISVZ of like-zone have the greatest similarity.

C, D Validation of microarray data by qRT–PCR (C) and ISH (D). ISH patterns were observed in three animals, at least three sections per animal, per gene. Plots are mean + SEM of relative fold level. Student's *t*-test, $*P < 0.05$, $**P < 0.01$, $***P < 0.001$. Statistical significance is indicated for qRT–PCR (black) and microarray (gray) data. Scale bar, 500 μm.

these gene expression patterns solely and specifically mapped the formation of functional areas A17 and A19, but it seemed to better support a general role on patterning the multiple folds and fissures.

In further support that modular expression may be relevant for the patterning of cortical folds, the above genes were not expressed in modular patterns in the developing mouse cortex (Fig 5B), where

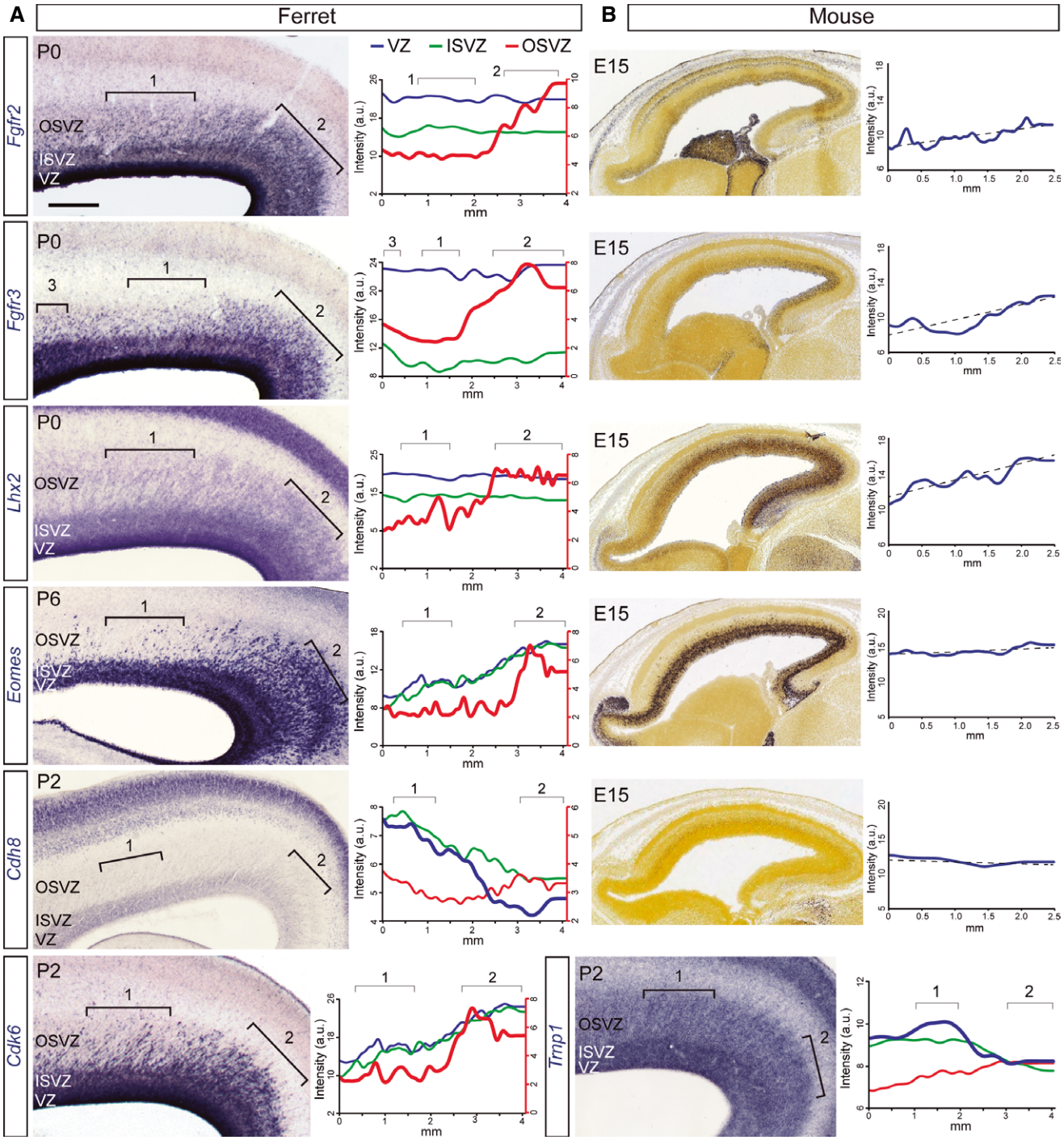

Figure 5. Modular patterns of mRNA expression in germinal layers delineate local protomaps.

A Patterns of ISH stain of DEGs across the occipital region of the ferret cortex at the indicated ages, and plots of stain intensity along each germinal layer (rostral is left, caudal is right; a.u., arbitrary units). For each gene, numbered brackets in graph correspond to the domains indicated in picture and identify the extent of adjacent domains with markedly distinct expression levels. Red *y*-axis is for red dataset, black *y*-axis is for all other datasets. For *Fgfr2*, *Fgfr3*, and *Lhx2*, expression in modules 1 and 2 is several-fold different along OSVZ but homogeneous along ISVZ and VZ. For *Eomes* and *Cdk6*, expression is higher in module 2 than in 1 in all layers, but changes are graded in VZ and ISVZ while abrupt in OSVZ. In contrast to other genes, *Cdh8* and *Trnp1* expression is higher in module 1 than in 2, changing abruptly along VZ, in a softer gradient along ISVZ, and homogeneous along OSVZ. ISH patterns were confirmed in three independent animals, at least three sections per animal, for each gene. Scale bar, 500 μm.

B Patterns of mRNA expression across the rostro-caudal extent of the mouse neocortex at embryonic day E15.5 (left is rostral, right is caudal), as of the Allen Brain Atlas (www.brain-map.org), and quantifications of ISH stain intensity along the rostro-caudal extent of the neocortex as in (A). Dashed lines are trend-line for the data plotted. While all genes are specifically expressed in germinal layers, intensity of gene expression is either homogeneous (*Eomes*, *Cdh8*) or in a shallow gradient across the entire rostro-caudal extent of the neocortex (*Fgfr2*, *Fgfr3*, *Lhx2*).

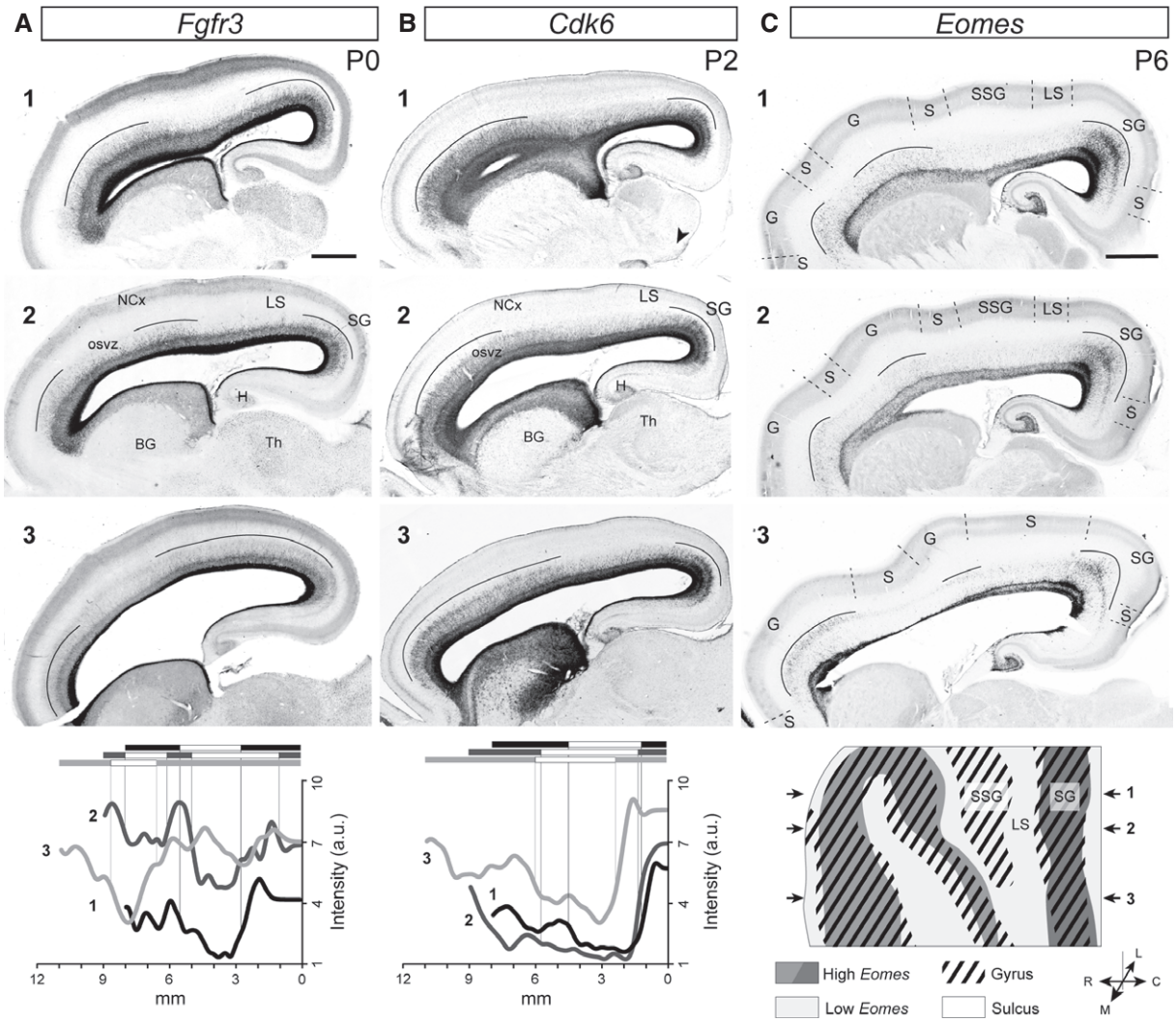

Figure 6. Maps of mRNA expression modules for *Fgfr3*, *Cdk6*, and *Eomes*.

A–C Low magnification images of sagittal sections of the ferret brain at postnatal day P0 (A), P2 (B), and P6 (C), showing the pattern of mRNA expression for *Fgfr3* (A), *Cdk6* (B), and *Eomes* (C). Graphs in (A) and (B) plot the stain intensity in OSVZ along the rostro-caudal extent of the neocortex (rostral is left, caudal is right) in each of the three consecutive latero-medial levels shown, as identified by numbers (1 = lateral, 3 = medial). Horizontal bars are binary representations of expression level along each section as in the line graph (each identified by a different shade of gray), indicating modules of overall high (gray) and low (white) expression. Plot in (C) is a map of the rostro-caudal and latero-medial extent of the cortex at P6, built from bar representations of consecutive sections as in (A, B). This map demonstrates strong spatial correlation between *Eomes* expression modules (shaded) and prospective gyri (striped pattern), with the only exception of the SSG. Dashed lines on pictures indicate the estimated border between prospective gyri (G) and sulci (S). The caudal vertex of the cortex, where *Eomes* expression is very high, will eventually expand to become the splenial gyrus (SG), flanked rostrally by the lateral sulcus (LS). Modules of high expression are indicated on pictures by continuous lines. BG, basal ganglia; C, caudal; H, hippocampus; L, lateral; LS, lateral sulcus; M, medial; NCx, neocortex; R, rostral; SG, splenial gyrus; Th, thalamus. Scale bars, 500 μm.

folds do not form, but multiple functional areas are distinguished (Sansom & Livesey, 2009; Elsen *et al*, 2013). Importantly, expression levels of *Eomes* in OSVZ correlated accurately with the map of cortical folding, with multiple high and low expression regions matching precisely with the emerging prospective folds and fissures (but not all) (Fig 6C). In contrast, other genes like *Fgfr3* or *Cdk6* only showed good correlation with SG and LS (Fig 6A and B). Taken together, our observations strongly suggested that modular gene expression may be a relevant feature underlying the formation of gyri and sulci, although the specific combination of genes involved is likely to vary between each gyrus and sulcus. In addition, as gyri and sulci frequently coincide with functional cortical areas, differential gene expression along germinal layers may also contribute to define prospective functional cortical areas in gyrencephalic species.

Expression of the modular protomap precedes cortical folding

Next, we enquired about the age of emergence and developmental progression of these modular protomaps. To address this, we compared the patterns of mRNA expression for *Eomes*, *Fgfr2*, *Fgfr3*, and *Cdk6* at three different developmental stages spanning the period of cortical neurogenesis in ferret: embryonic day 30 (E30),

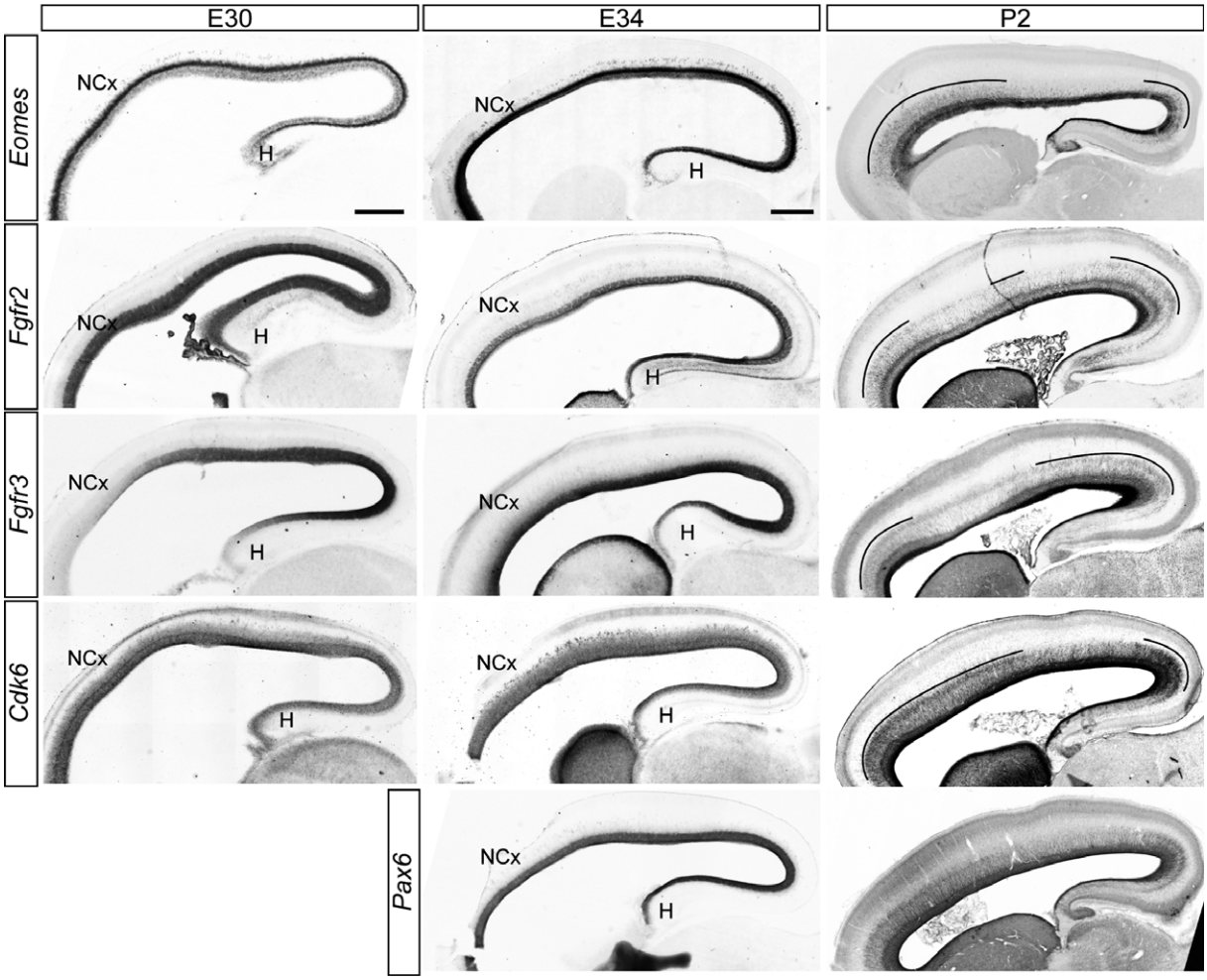

Figure 7. Late protomap formation precedes cortical folding.
Patterns of mRNA expression for *Eomes*, *Fgfr2*, *Fgfr3*, *Cdk6*, and *Pax6* across the rostro-caudal extent of the neocortex at E30, E34, and P2. Lines indicate discrete domains of high expression in OSVZ. At E30 and E34, all genes tested were homogeneously expressed, and only by P2 modules of high versus low expression were distinguishable. Patterns were observed in at least three sections per animal, one to three animals per stain. H, hippocampus. Scale bars, 500 μm.

E34 and P2 (Jackson *et al*, 1989). At E30, gene expression was homogeneous across the entire rostro-caudal extent of the cortical primordium except for *Fgfr3*, which displayed a long-spanning gradient low rostral-high caudal, similar to the patterns observed in the lissencephalic mouse embryo (Figs 5B and 7). Importantly, we found no indication of modular gene expression at this early stage. At E34, gene expression continued to be completely homogeneous across the cortical primordium, even for *Fgfr3* which did not show its early gradient anymore. The domains or modules of gene expression only became distinguishable in early postnatal ferrets, and particularly in the OSVZ (Fig 7). Interestingly, although these modular patterns emerged perinatally for all genes examined, the age at which expression modules or domains were most distinct varied depending on each gene (Figs 6 and 7). Further highlighting the potential relevance of *Eomes* in cortical patterning and folding, this gene displayed the greatest refinement in expression pattern and contrast between modules circa P6, the onset age for gyrus formation (Smart & McSherry, 1986a). Given that *Eomes* controls the expression of multiple cortical patterning genes (Sessa *et al*, 2008; Sansom & Livesey, 2009; Elsen *et al*, 2013), and its mutation in humans causes severe cortical folding defects (Baala *et al*, 2007), this could be an important gene in patterning cortical folds, as it has been shown to participate in the sequential definition of cortical patterning in mouse (Elsen *et al*, 2013).

Human cortical malformation genes are also expressed in discrete domains

Cross-examination of our microarray data with public databases (Barkovich *et al*, 2012) revealed that 81% of genes mutated in human syndromes of cortical malformation are DEGs between ferret SG and LS ($P < 0.05$, FC ≥ 1.25; Supplementary Table S6). Importantly, many of these human malformations frequently only affect a discrete region, while sparing the rest of the cerebral cortex, such as those emerging from mutations in *FGFR3*, *FLNA*, or *GPR56* (Fox *et al*, 1998; Piao *et al*, 2004; Hevner, 2005). We tested whether these genes causing regional malformations in humans and found differentially expressed between prospective SG and LS in the ferret cortex, might

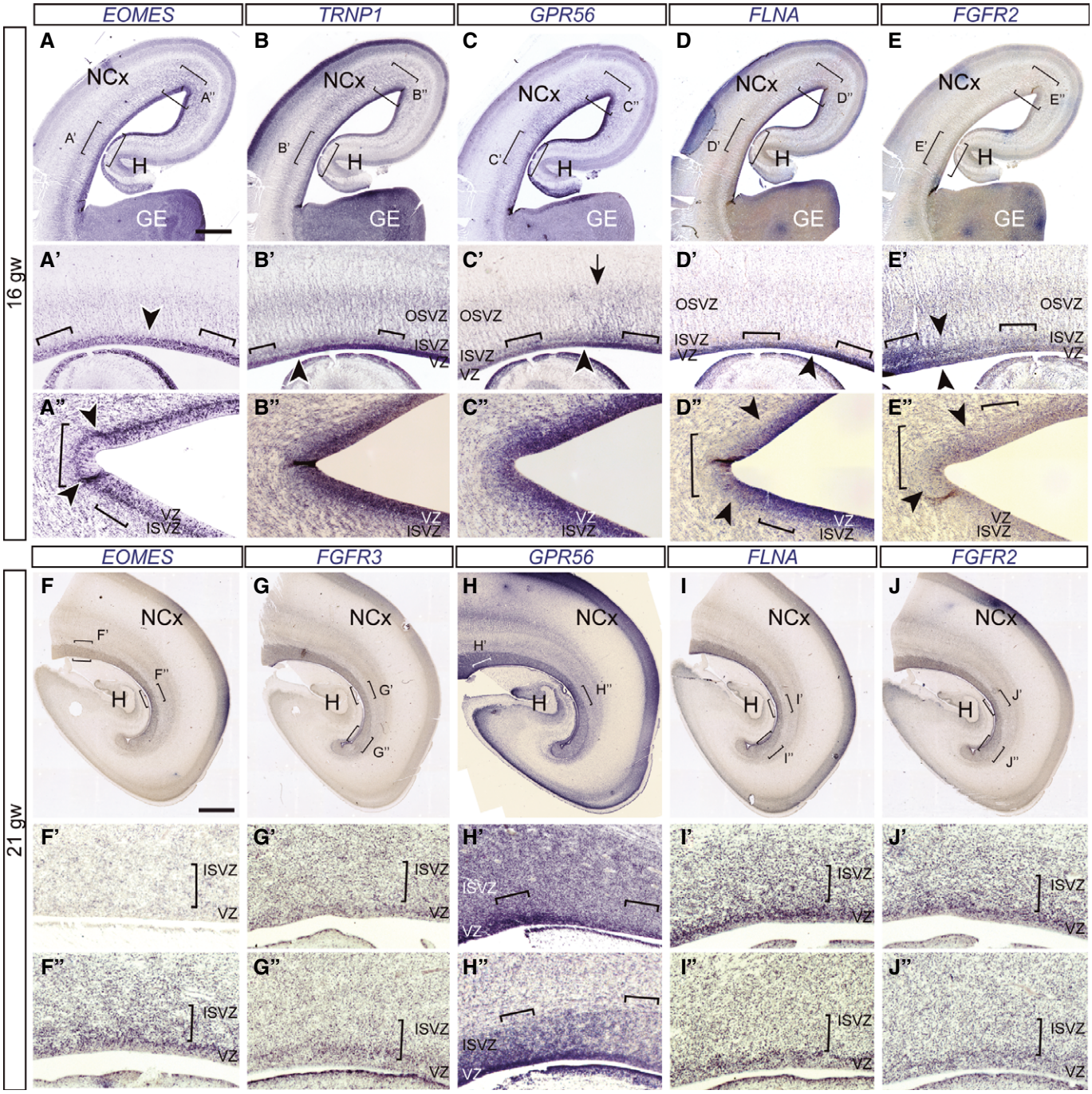

Figure 8. Modular patterns of gene expression in the developing cortex of human embryos.

A–E″ Patterns of mRNA expression for the indicated genes in the developing cerebral cortex of human embryos at 16 gestational weeks (gw). Brackets in (A–E) indicate the location of details shown in (A′–E″). In detail pictures, arrowheads and arrows indicate points of abrupt change in mRNA levels or distribution, and pairs of brackets indicate regions with significantly different levels of ISH stain along VZ (A′, A″ , B′ ,C′ ,C′ ,D″ ,E′, E″). Scale bar, 1 mm.

F–J″ Patterns of mRNA expression for the indicated genes in the developing cerebral cortex of human embryos at 21 gw. Brackets in (F–J) indicate the location of details shown in (F′–J″). In detail pictures, pairs of brackets indicate regions with significantly different levels along ISVZ (F′, F″; G′, G″; H′; H″; I′, I″; J′, J″). Changes in *FGFR2* and *FGFR3* expression were obvious in VZ at 16 gw, and in ISVZ at 21 gw. NCx, neocortex; GE, ganglionic eminence; H, hippocampus. Scale bar, 2 mm.

be expressed in regional or modular patterns also in the human cortex at fetal stages. We performed ISH stains on brain sections from human embryos at 16 and 21 gestational weeks (gw), which correspond to stages of mid- and late neurogenesis and immediately prior to the emergence of the first folds and fissures. Thus, analysis of these stages should help us define the genetic profile of germinal layers preceding the appearance of the cortical folds. We found significant regional variations in expression levels for all genes

tested. These included the existence of significant changes at short-range in mRNA expression levels for several genes known to be key in cortical folding, such as EOMES, TRNP1, and GPR56 (Piao *et al*, 2004; Baala *et al*, 2007; Stahl *et al*, 2013; Bae *et al*, 2014) locally within the prospective prefrontal cortex and frontal lobe (Fig 8A–E), as well as within the ventral temporal lobe (Fig 8F–J).

Discussion

Recent landmark studies using whole-tissue and single-cell RNA sequencing have identified a reduced number of genes with key importance in human-specific cortical expansion and progenitor cell heterogeneity (Lui *et al*, 2014; Florio *et al*, 2015; Johnson *et al*, 2015). But in large-brained mammals like humans, macaques, and ferrets, the embryonic cerebral cortex is highly regionalized, including the formation of folds and fissures (Welker, 1990), and many of the critical features defining cortical progenitor cells (cell cycle, amplification, neurogenesis) vary significantly across such regions (Dehay *et al*, 1993; Lukaszewicz *et al*, 2005; Dehay & Kennedy, 2007; Reillo *et al*, 2011). Here, we have compared for the first time the transcriptomes of germinal layers between prospective folds and fissures of the developing cerebral cortex and described the existence of a novel pattern of gene expression along these germinal layers. For an identified subset of developmentally relevant genes, we find that expression levels change abruptly and repeatedly across the cortex, distinguishing multiple domains or modules with differential gene expression (differentially expressed genes, DEGs). Importantly, these multi-modular patterns of expression are found in the developing cortex of gyrencephalic species (ferret and human), but not in the lissencephalic cortex of mouse (Sansom & Livesey, 2009; Elsen *et al*, 2013).

In agreement with the remarkable size and complexity of the OSVZ in gyrencephalic species, a majority of DEGs are found along this layer, and gene expression modules along the OSVZ map faithfully the eventual location of cortical folds and fissures. This supports a role for this layer and some of our identified DEGs on cortical patterning, including the stereotyped formation of folds (Kriegstein *et al*, 2006; Lui *et al*, 2011; Reillo *et al*, 2011). Indeed, many of the genes we found differentially expressed between the prospective splenial gyrus and lateral sulcus are known to regulate progenitor proliferation, neurogenesis, or fate specification. These include key signaling pathways such as Notch, Shh, MAPK, and Wnt, which directly regulate cortical growth (Lui *et al*, 2011; Reillo *et al*, 2011; Barkovich *et al*, 2012; Nonaka-Kinoshita *et al*, 2013; Rash *et al*, 2013; Borrell & Gotz, 2014). Taken together, our data fit with the cortical protomap concept to pattern the cerebral cortex primordium into prospective anatomical and functional regions (Rakic, 1988). In the case of cortical folds, modular patterns of expression for a combination of genes, possibly different depending on the specific gyrus and sulcus, may impose differential tissue growth between modules, eventually leading to the evagination of the cortex and formation of folds (Smart & McSherry, 1986b).

Our findings demonstrate that differential gene expression along the OSVZ fits well with the patterning of cortical folds. Nevertheless, folds and fissures in the cerebral cortex frequently coincide with functional areas. For example, the SG coincides with visual area A17, and LS coincides with area A19 of the visual cortex. Hence, it seems arguable that the modules of gene expression we have identified may reflect a more complex regulation of cortical maps in gyrencephalic species, instead of patterning folds. The repeated variations in gene expression level that germinal layers display across the ferret and human cortex seem contrary to defining the identity of a particular area, but better fit with defining a systematically repeated feature across the cortex, such as folds and fissures. This notion is further substantiated by our comparisons between mouse and ferret cortex: gene expression in mouse germinal layers is nearly always homogeneous or in very shallow gradients, including genes which in ferret are expressed in distinct modular patterns. Given that both mouse and ferret form cortical areas, but only ferret forms folds, this again supports a role for genetic modularity in cortical folding, or a much more complex regulation of cortical area patterning than in mouse (Sansom & Livesey, 2009; Elsen *et al*, 2013).

Importantly, previous reports had already demonstrated that locally manipulating the expression level of some of our DEGs has a significant impact on the size and shape of cortical folds, but without altering cortical area identity nor lamination (Reillo *et al*, 2011; Nonaka-Kinoshita *et al*, 2013; Stahl *et al*, 2013; Borrell & Gotz, 2014). Nevertheless, our current analysis also demonstrates the existence of DEGs and step-wise expression changes in VZ and ISVZ of ferret and human, indicating that multiple genetic maps overlap across cortical germinal layers. Because VZ and ISVZ are major sites of neurogenesis and neural fate determination in ferret (Reillo *et al*, 2011), gene expression patterns in these other layers may contribute significantly to define functional areas of the cerebral cortex.

Our dataset of differentially expressed genes between prospective folds and fissures is a unique resource to investigate the genetic regulation of cortical folding (Borrell & Gotz, 2014). Importantly, our screen highlights over 80% of the genes mutated in human cortical malformations (Barkovich *et al*, 2012), some of which are also expressed in modules along germinal layers of the developing cerebral cortex of both ferret and human fetuses. This highlights the promise of this screen as an entry point to identify novel genes mutated in human malformations of cortical development.

Materials and Methods

Animals and tissue processing

Pregnant pigmented ferrets (*Mustela putorius furo*) were obtained from Marshall Bioresources (North Rose, NY) and kept on a 1-h 6:8-h light:dark cycle at the Animal Facilities of the Universidad Miguel Hernández. All animals were treated according to Spanish and EU regulations, and experimental protocols were approved by the Universidad Miguel Hernández IACUC. Bromodeoxyuridine (BrdU, SIGMA) was administered intraperitoneally at 50 mg/kg 1 h prior to sacrifice. For histological analysis, ferret embryos were obtained by cesarean section of timed-pregnant females upon deep anesthesia with sodium pentobarbital and then perfused transcardially with 4% paraformaldehyde (PFA); postnatal ferrets were deeply anesthetized with sodium pentobarbital prior to transcardiac perfusion with PFA. After perfusion, the brains were extracted, cryoprotected, frozen, and sectioned.

Tissue microdissection

For RNA extraction, ferret pups were anesthetized and decapitated; their brains were dissected and blocked in ice-cold ACSF (140 mM NaCl, 5 mM KCl, 1 mM $MgCl_2$, 24 mM D-glucose, 10 mM HEPES, 1 mM $CaCl_2$, pH 7.2), and tissue blocks containing the occipital cortex were vibrotome-cut in 300-μm-thick slices. Living cortical slices were further microdissected with microscalpels in ice-cold ACSF to isolate the VZ, ISVZ, and OSVZ from the prospective splenial gyrus and lateral sulcus. We identified the SG as the region corresponding to the caudal end of the cortex, where it curves back; LS was identified as the cortical region overlying the hippocampus at the level of the dentate gyrus. Germinal layers were identified in living slices under the dissection scope: the VZ was the most opaque layer, on the apical side of the cortex; the ISVZ was less opaque than VZ, but with a visibly higher cell density than the overlying layers. Between the cell-dense ISVZ and CP, there was a very translucent and thick zone, corresponding to OSVZ+IZ+SP; the OSVZ was identified as the bottom half of this zone, which usually had a higher cell density than IZ/SP, particularly at the level of the SG. Tissue pieces were fresh-frozen in Trizol for RNA extraction, with a post-mortem interval of < 1 h.

Human tissue

Brain sections of human fetuses from spontaneous abortions were obtained from the Service of Pathology, Hospital Universitario "Principe de Asturias", Alcalá de Henares, Spain. Brains were removed in routine necropsies in accordance with the Spanish law on clinical autopsies (Boletín Oficial del Estado [BOE] of 27 June 1980 and BOE of 11 September 1982). After removal, brains were fixed by immersion in buffered 4% paraformaldehyde (PFA) at room temperature during 2 weeks. Then, coronal blocks across the entire brain were obtained; these blocks were embedded *in toto* in paraffin, and finally sectioned and stained.

RNA isolation, processing, and microarray hybridization

Total RNA was extracted using RNeasy Mini Kit (Quiagen) followed by treatment with RNase-Free DNase Set (Quiagen). RNA quality was confirmed using the RNA 6000 Nano kit on the Agilent Bioanalyzer platform, and then 200 ng of total RNA was labeled using the one-color labeling kit from Agilent technologies according to the manufacturer's protocol. Labeled cRNA was then hybridized for 16 h on a custom-made microarray containing 43,692 ferret-specific probes covering 17,386 genes (Camp *et al*, 2012). Microarray slides were scanned on an Agilent High-Resolution C Scanner, and the raw image files were processed by the Agilent feature extraction software. Raw data files were normalized using quantile normalization in Partek Genomics Suite®. Statistical analysis of microarray data was done in Multiexperiment Viewer (MEV) (Saeed *et al*, 2003). To identify genes with significantly different expression levels, we used ANOVA comparisons between samples, using *P*-values based on 500 permutations and Bonferroni false discovery correction, as in Ayoub *et al* (2011). Microarray comparison of samples between SG and LS revealed that in OSVZ, the majority of differentially expressed genes (DEGs) were up-regulated in SG. Although it was intuitive to assume that normalization of mRNA abundance should have resulted in roughly 50% of DEGs up-regulated and 50% down-regulated, DEGs in OSVZ only represented 6.9% of genes, and their average degree of change was only 2.9-fold. Therefore, the impact of this difference on the total amount of RNA in the biological samples was very likely negligible, particularly when many DEGs were transcription factors, cell cycle proteins, etc., typically having a low abundance overall. The microarray data from this publication have been submitted to the GEO database (http://www.ncbi.nlm.nih.gov/geo/) and assigned the identifier GSE60687.

Gene ontology analysis

Annotation analysis was performed using the web-based DAVID v6.7 software (http://david.abcc.ncifcrf.gov) (Dennis *et al*, 2003). When comparing areas, common terms were selected among the categories with highest enrichment score. In order to find the functional terms specific for each layer, annotation terms common with the other layers were removed from the final output in each case. Functional annotation clustering for DEGs between layers was done in the same way.

Quantitative real-time PCR

Total RNA from each region of interest was isolated by microdissection following the same procedures as for microarray analysis, and primers for ferret gene homologs were designed based on the same ferret-specific sequences. Template cDNA was generated using Maxima First Strand cDNA Synthesis Kit for quantitative real-time PCR (qRT–PCR) (Thermo Fisher). Quantitative RT–PCR was performed using the Step One Plus sequence detection system and the SYBR Green method (Applied Biosystems), with each point examined in triplicate. Transcript levels were calculated using the comparative C_t method normalized using actin. Primers used are listed in Supplementary Table S2 (actin primers used by Fang and colleagues) (Fang *et al*, 2010). Each independent sample was assayed in duplicate. Data were statistically analyzed with SPSS software using *t*-test. Histograms represent mean ± SEM.

Cloning of ferret gene homologs

Several DEGs were amplified by PCR using ferret-specific primers, designed based on the same ferret-specific sequences as in the microarray, and listed in Supplementary Table S2. PCR was performed using Go Taq Flexi DNA polymerase (Promega), and the resulting amplicons were purified with Wizard SV Gel and PCR Clean-Up System (Promega) and cloned into pGEM-T Easy Vector System I.

In situ hybridization and immunohistochemistry

Sense and anti-sense cRNA probes were synthesized and labeled with digoxigenin (DIG; Roche Diagnostics) according to the manufacturer's instructions. *In situ* hybridization (ISH) was performed as described elsewhere (Reillo *et al*, 2011). Briefly, 50-μm-thick frozen brain sections were hybridized with DIG-labeled cRNA probes overnight in hybridization solution [50% formamide (Ambion), 10% dextran sulfate, 0.2% tRNA (Invitrogen), 1× Denhardt's solution (from a 50× stock; SIGMA), 1× salt solution (containing 0.2 M NaCl, 0.01 M Tris, 5 mM NaH_2PO_4, 5 mM Na_2HPO_4, 5 mM EDTA, pH 7.5)]. After sections were washed,

alkaline phosphatase-coupled anti-digoxigenin Fab fragments were applied. For visualization of the labeled cRNAs, sections were incubated in nitroblue tetrazolium (NBT)/5-bromo-4-chloro-3-indolyl phosphate (BCIP) solution [3.4 μl/ml from NBT stock and 3.5 μl/ml from BCIP stock in reaction buffer (100 mg/ml NBT stock in 70% dimethylformamide; 50 mg/ml BCIP stock in 100% dimethylformamide; Roche)]. Ferret-specific ISH probes were cloned using the primers listed in Supplementary Table S2. The following plasmids for human ISH were purchased from "Source BioScience LifeSciences" (http://www.lifesciences.sourcebioscience.com/), with their respective Clone ID: EOMES (5223017), FGFR2 (5264983), FGFR3 (40122516), FLNA (4800733), GPR56 (3139174), and TRNP1 (6376829). For immunohistochemistry, brain sections were incubated with primary antibodies overnight (anti-BrdU, 1:200; anti-Tbr2, 1:250; Abcam), followed by biotinylated secondary antibodies (1:250, Vector), ABC complex (1:100, Dako) and developed with nickel-enhanced diaminobenzidine (SIGMA).

Generation of cortical maps

Gene expression patterns were categorized as being modular when this was observed in three independent animals, at least three sections per animal, for each gene. To map the distribution of gene expression levels across the developing cortex, a series of sagittal sections across the latero-medial extent of the cortex were stained for ISH. In each section, the apical border of the OSVZ was drawn, and this line was subdivided marking regions with high or low intensity of stain, and straightened. The entire set of straight lines was ordered medio-laterally, aligned to the caudal end, and "high" or "low" sectors across sections were grouped in two-dimensional territories following best-likelihood criteria. To map prospective folds and fissures, we followed the exact same process, but dividing the apical border of OSVZ from each section into regions prospective of gyrus or sulcus. The borders between gyrus and sulcus regions were defined as the points of change in convexity at the cortical surface, which were then projected perpendicularly onto the apical border of the OSVZ.

Generation of ISH intensity plots

Quantification of ISH intensity along the OSVZ, ISVZ, or VZ was performed using ImageJ. Images of ISH stains were converted to 8-bit and contrast-enhanced, and the entire thickness of OSVZ, ISVZ, or VZ was selected and straightened using the straighten plugin (http://rsbweb.nih.gov/ij/plugins/straighten.html). This region of interest was then analyzed for pixel intensity using Plot Profile along the length of the OSVZ, and raw data across individual points were smoothed to reveal the intensity trend.

Supplementary information for this article is available online: http://emboj.embopress.org

Acknowledgements

We thank C. Vegar and E. Picó for technical assistance; F. Heredia for assistance with qRT–PCR, Olga Díez Jambrina (Service of Pathology, Hospital Universitario "Principe de Asturias", Alcalá de Henares, Spain) for help in processing embryonic human tissue; C. Redies for ferret *Cdh8* ISH probe; and M.A. Nieto and N. Papalopulu for critical reading of the manuscript. CdJR was in part recipient of "Juan de la Cierva" fellowship from the Spanish Ministry of Science and Innovation (MICINN), and Fundación Alicia Koplowitz fellowship. The research leading to a part of these results received funding from the European Union Seventh Framework Programme FP7/2007–2013 under the project DESIRE (grant agreement no. 602531), MICINN (SAF2009-07367), the Spanish Ministry of Economy and Competitivity (BFU2012-33473, CSD2007-00023) and European Research Council (ERC StG309633) to VB. The Instituto de Neurociencias is a "Centre of Excellence Severo Ochoa".

Author contributions

CdJR and VB designed work; CdJR, CB, and UT performed experiments; JMSA provided human samples; and VB provided reagents and analytic tools, supervised work and wrote manuscript.

Conflict of interest

The authors declare that they have no conflict of interest.

References

Ayoub AE, Oh S, Xie Y, Leng J, Cotney J, Dominguez MH, Noonan JP, Rakic P (2011) Transcriptional programs in transient embryonic zones of the cerebral cortex defined by high-resolution mRNA sequencing. *Proc Natl Acad Sci U S A* 108: 14950 – 14955

Baala L, Briault S, Etchevers HC, Laumonnier F, Natiq A, Amiel J, Boddaert N, Picard C, Sbiti A, Asermouh A, Attie-Bitach T, Encha-Razavi F, Munnich A, Sefiani A, Lyonnet S (2007) Homozygous silencing of T-box transcription factor EOMES leads to microcephaly with polymicrogyria and corpus callosum agenesis. *Nat Genet* 39: 454 – 456

Bae BI, Tietjen I, Atabay KD, Evrony GD, Johnson MB, Asare E, Wang PP, Murayama AY, Im K, Lisgo SN, Overman L, Sestan N, Chang BS, Barkovich AJ, Grant PE, Topcu M, Politsky J, Okano H, Piao X, Walsh CA (2014) Evolutionarily dynamic alternative splicing of GPR56 regulates regional cerebral cortical patterning. *Science* 343: 764 – 768

Barkovich AJ, Guerrini R, Kuzniecky RI, Jackson GD, Dobyns WB (2012) A developmental and genetic classification for malformations of cortical development: update 2012. *Brain* 135: 1348 – 1369

Betizeau M, Cortay V, Patti D, Pfister S, Gautier E, Bellemin-Menard A, Afanassieff M, Huissoud C, Douglas RJ, Kennedy H, Dehay C (2013) Precursor diversity and complexity of lineage relationships in the outer subventricular zone of the primate. *Neuron* 80: 442 – 457

Bishop KM, Goudreau G, O'Leary DD (2000) Regulation of area identity in the mammalian neocortex by Emx2 and Pax6. *Science* 288: 344 – 349

Borrell V, Reillo I (2012) Emerging roles of neural stem cells in cerebral cortex development and evolution. *Dev Neurobiol* 72: 955 – 971

Borrell V, Gotz M (2014) Role of radial glial cells in cerebral cortex folding. *Curr Opin Neurobiol* 27C: 39 – 46

Camp JV, Svensson TL, McBrayer A, Jonsson CB, Liljestrom P, Bruder CE (2012) De-novo transcriptome sequencing of a normalized cDNA pool from influenza infected ferrets. *PLoS ONE* 7: e37104

Chou SJ, Perez-Garcia CG, Kroll TT, O'Leary DD (2009) Lhx2 specifies regional fate in Emx1 lineage of telencephalic progenitors generating cerebral cortex. *Nat Neurosci* 12: 1381 – 1389

Dehay C, Giroud P, Berland M, Smart I, Kennedy H (1993) Modulation of the cell cycle contributes to the parcellation of the primate visual cortex. *Nature* 366: 464 – 466

Dehay C, Kennedy H (2007) Cell-cycle control and cortical development. *Nat Rev Neurosci* 8: 438 – 450

Dennis G Jr, Sherman BT, Hosack DA, Yang J, Gao W, Lane HC, Lempicki RA (2003) DAVID: database for annotation, visualization, and integrated discovery. *Genome Biol* 4: P3

Elsen GE, Hodge RD, Bedogni F, Daza RA, Nelson BR, Shiba N, Reiner SL, Hevner RF (2013) The protomap is propagated to cortical plate neurons through an Eomes-dependent intermediate map. *Proc Natl Acad Sci U S A* 110: 4081 – 4086

Fang Y, Rowe T, Leon AJ, Banner D, Danesh A, Xu L, Ran L, Bosinger SE, Guan Y, Chen H, Cameron CC, Cameron MJ, Kelvin DJ (2010) Molecular characterization of in vivo adjuvant activity in ferrets vaccinated against influenza virus. *J Virol* 84: 8369 – 8388

Fietz SA, Kelava I, Vogt J, Wilsch-Brauninger M, Stenzel D, Fish JL, Corbeil D, Riehn A, Distler W, Nitsch R, Huttner WB (2010) OSVZ progenitors of human and ferret neocortex are epithelial-like and expand by integrin signaling. *Nat Neurosci* 13: 690 – 699

Fietz SA, Huttner WB (2011) Cortical progenitor expansion, self-renewal and neurogenesis-a polarized perspective. *Curr Opin Neurobiol* 21: 23 – 35

Fietz SA, Lachmann R, Brandl H, Kircher M, Samusik N, Schroder R, Lakshmanaperumal N, Henry I, Vogt J, Riehn A, Distler W, Nitsch R, Enard W, Paabo S, Huttner WB (2012) Transcriptomes of germinal zones of human and mouse fetal neocortex suggest a role of extracellular matrix in progenitor self-renewal. *Proc Natl Acad Sci U S A* 109: 11836 – 11841

Florio M, Albert M, Taverna E, Namba T, Brandl H, Lewitus E, Haffner C, Sykes A, Wong FK, Peters J, Guhr E, Klemroth S, Prufer K, Kelso J, Naumann R, Nusslein I, Dahl A, Lachmann R, Paabo S, Huttner WB (2015) Human-specific gene ARHGAP11B promotes basal progenitor amplification and neocortex expansion. *Science* 347: 1465 – 1470

Fox JW, Lamperti ED, Eksioglu YZ, Hong SE, Feng Y, Graham DA, Scheffer IE, Dobyns WB, Hirsch BA, Radtke RA, Berkovic SF, Huttenlocher PR, Walsh CA (1998) Mutations in filamin 1 prevent migration of cerebral cortical neurons in human periventricular heterotopia. *Neuron* 21: 1315 – 1325

Gotz M, Huttner WB (2005) The cell biology of neurogenesis. *Nat Rev Mol Cell Biol* 6: 777 – 788

Hevner RF (2005) The cerebral cortex malformation in thanatophoric dysplasia: neuropathology and pathogenesis. *Acta Neuropathol* 110: 208 – 221

Hobert O (2011) Regulation of terminal differentiation programs in the nervous system. *Annu Rev Cell Dev Biol* 27: 681 – 696

Jackson CA, Peduzzi JD, Hickey TL (1989) Visual cortex development in the ferret. I. Genesis and migration of visual cortical neurons. *J Neurosci* 9: 1242 – 1253

Jessell TM (2000) Neuronal specification in the spinal cord: inductive signals and transcriptional codes. *Nat Rev Genet* 1: 20 – 29

Johnson MB, Wang PP, Atabay KD, Murphy EA, Doan RN, Hecht JL, Walsh CA (2015) Single-cell analysis reveals transcriptional heterogeneity of neural progenitors in human cortex. *Nat Neurosci* 18: 637 – 646

Kriegstein A, Noctor S, Martinez-Cerdeno V (2006) Patterns of neural stem and progenitor cell division may underlie evolutionary cortical expansion. *Nat Rev Neurosci* 7: 883 – 890

Law MI, Zahs KR, Stryker MP (1988) Organization of primary visual cortex (area 17) in the ferret. *J Comp Neurol* 278: 157 – 180

Lui JH, Hansen DV, Kriegstein AR (2011) Development and evolution of the human neocortex. *Cell* 146: 18 – 36

Lui JH, Nowakowski TJ, Pollen AA, Javaherian A, Kriegstein AR, Oldham MC (2014) Radial glia require PDGFD-PDGFRbeta signalling in human but not mouse neocortex. *Nature* 515: 264 – 268

Lukaszewicz A, Savatier P, Cortay V, Giroud P, Huissoud C, Berland M, Kennedy H, Dehay C (2005) G1 phase regulation, area-specific cell cycle control, and cytoarchitectonics in the primate cortex. *Neuron* 47: 353 – 364

Mangale VS, Hirokawa KE, Satyaki PR, Gokulchandran N, Chikbire S, Subramanian L, Shetty AS, Martynoga B, Paul J, Mai MV, Li Y, Flanagan LA, Tole S, Monuki ES (2008) Lhx2 selector activity specifies cortical identity and suppresses hippocampal organizer fate. *Science* 319: 304 – 309

Manger PR, Kiper D, Masiello I, Murillo L, Tettoni L, Hunyadi Z, Innocenti GM (2002) The representation of the visual field in three extrastriate areas of the ferret (*Mustela putorius*) and the relationship of retinotopy and field boundaries to callosal connectivity. *Cereb Cortex* 12: 423 – 437

Molyneaux BJ, Arlotta P, Menezes JR, Macklis JD (2007) Neuronal subtype specification in the cerebral cortex. *Nat Rev Neurosci* 8: 427 – 437

Nonaka-Kinoshita M, Reillo I, Artegiani B, Martinez-Martinez MA, Nelson M, Borrell V, Calegari F (2013) Regulation of cerebral cortex size and folding by expansion of basal progenitors. *EMBO J* 32: 1817 – 1828

Nord AS, Blow MJ, Attanasio C, Akiyama JA, Holt A, Hosseini R, Phouanenavong S, Plajzer-Frick I, Shoukry M, Afzal V, Rubenstein JL, Rubin EM, Pennacchio LA, Visel A (2013) Rapid and pervasive changes in genome-wide enhancer usage during mammalian development. *Cell* 155: 1521 – 1531

Pattabiraman K, Golonzhka O, Lindtner S, Nord AS, Taher L, Hoch R, Silberberg SN, Zhang D, Chen B, Zeng H, Pennacchio LA, Puelles L, Visel A, Rubenstein JL (2014) Transcriptional regulation of enhancers active in protodomains of the developing cerebral cortex. *Neuron* 82: 989 – 1003

Piao X, Hill RS, Bodell A, Chang BS, Basel-Vanagaite L, Straussberg R, Dobyns WB, Qasrawi B, Winter RM, Innes AM, Voit T, Ross ME, Michaud JL, Descarie JC, Barkovich AJ, Walsh CA (2004) G protein-coupled receptor-dependent development of human frontal cortex. *Science* 303: 2033 – 2036

Rakic P (1988) Specification of cerebral cortical areas. *Science* 241: 170 – 176

Rash BG, Tomasi S, Lim HD, Suh CY, Vaccarino FM (2013) Cortical gyrification induced by fibroblast growth factor 2 in the mouse brain. *J Neurosci* 33: 10802 – 10814

Reillo I, de Juan Romero C, Garcia-Cabezas MA, Borrell V (2011) A role for intermediate radial glia in the tangential expansion of the Mammalian cerebral cortex. *Cereb Cortex* 21: 1674 – 1694

Reillo I, Borrell V (2012) Germinal zones in the developing cerebral cortex of ferret: ontogeny, cell cycle kinetics, and diversity of progenitors. *Cereb Cortex* 22: 2039 – 2054

Saeed AI, Sharov V, White J, Li J, Liang W, Bhagabati N, Braisted J, Klapa M, Currier T, Thiagarajan M, Sturn A, Snuffin M, Rezantsev A, Popov D, Ryltsov A, Kostukovich E, Borisovsky I, Liu Z, Vinsavich A, Trush V *et al* (2003) TM4: a free, open-source system for microarray data management and analysis. *Biotechniques* 34: 374 – 378

Sahara S, Kawakami Y, Izpisua Belmonte JC, O'Leary DD (2007) Sp8 exhibits reciprocal induction with Fgf8 but has an opposing effect on anterior-posterior cortical area patterning. *Neural Dev* 2: 10

Sansom SN, Livesey FJ (2009) Gradients in the brain: the control of the development of form and function in the cerebral cortex. *Cold Spring Harb Perspect Biol* 1: a002519

Sessa A, Mao CA, Hadjantonakis AK, Klein WH, Broccoli V (2008) Tbr2 directs conversion of radial glia into basal precursors and guides neuronal amplification by indirect neurogenesis in the developing neocortex. *Neuron* 60: 56 – 69

Smart IH, McSherry GM (1986a) Gyrus formation in the cerebral cortex in the ferret. I. Description of the external changes. *J Anat* 146: 141 – 152

Smart IH, McSherry GM (1986b) Gyrus formation in the cerebral cortex of the ferret. II. Description of the internal histological changes. *J Anat* 147: 27 – 43

Smart IH, Dehay C, Giroud P, Berland M, Kennedy H (2002) Unique morphological features of the proliferative zones and postmitotic compartments of the neural epithelium giving rise to striate and extrastriate cortex in the monkey. *Cereb Cortex* 12: 37 – 53

Stahl R, Walcher T, De Juan Romero C, Pilz GA, Cappello S, Irmler M, Sanz-Aquela JM, Beckers J, Blum R, Borrell V, Gotz M (2013) Trnp1 regulates expansion and folding of the mammalian cerebral cortex by control of radial glial fate. *Cell* 153: 535 – 549

Visel A, Taher L, Girgis H, May D, Golonzhka O, Hoch RV, McKinsey GL, Pattabiraman K, Silberberg SN, Blow MJ, Hansen DV, Nord AS, Akiyama JA, Holt A, Hosseini R, Phouanenavong S, Plajzer-Frick I, Shoukry M, Afzal V, Kaplan T *et al* (2013) A high-resolution enhancer atlas of the developing telencephalon. *Cell* 152: 895 – 908

Welker W (1990) Why does cerebral cortex fissure and fold? A review of determinants of gyri and sulci. In *Cerebral Cortex, Peters A*, Jones EG (eds), Vol. 8B, pp 3 – 136. New York and London: Plenum Press

Yun K, Potter S, Rubenstein JL (2001) Gsh2 and Pax6 play complementary roles in dorsoventral patterning of the mammalian telencephalon. *Development* 128: 193 – 205

